Fine-mapping and identification of candidate causal genes for tail length in the Merinolandschaf breed

Dominik Karl Lagler[1,2], Elisabeth Hannemann[1], Kim Eck[1,2], Jürgen Klawatsch[1,2], Doris Seichter[2], Ingolf Russ[2], Christian Mendel[3], Gesine Lühken[4], Stefan Krebs[5], Helmut Blum[5], Maulik Upadhyay[1], Ivica Medugorac[1*]

[1] Population Genomics Group, Department of Veterinary Sciences, LMU Munich, Lena-Christ-Str. 48, 82152 Martinsried, Germany

[2] Tierzuchtforschung e.V. München, Senator-Gerauer-Str. 23, 85586 Poing, Germany

[3] Institute for Animal Breeding, Bavarian State Research Center for Agriculture, Prof.-Dürrwaechter-Platz 1, 85586 Poing, Germany

[4] Department of Animal Breeding and Genetics, JLU Gießen, Ludwigstr. 21a, 35390 Gießen, Germany

[5] Laboratory for Functional Genome Analysis, Gene Center, Ludwig-Maximilians-University Munich, 80539 Munich, Germany

* Corresponding author: Dr. Ivica Medugorac

Email address: i.medugorac@lmu.de

Phone: +49(0)89/2180-3310

Fax: +49(0)89/2180-99-3310

Email addresses:

DL: Dominik.Lagler@gen.vetmed.uni-muenchen.de

EH: Elisabeth.Kunz@gen.vetmed.uni-muenchen.de

KE: Kim.Eck@gen.vetmed.uni-muenchen.de

JK: Juergen.Klawatsch@gen.vetmed.uni-muenchen.de

DS: Doris.Seichter@tzfgen-bayern.de

IG: Ingolf.Russ@tzfgen-bayern.de

CM: Christian.Mendel@lfl.bayern.de

GL: Gesine.Luehken@agrar.uni-giessen.de

SK: Krebs@genzentrum.lmu.de

HB: Blum@genzentrum.lmu.de

MU: U.Maulik@gen.vetmed.uni-muenchen.de

Abstract

Background

Docking the tails of young lambs in long-tailed sheep breeds is a common practice worldwide. This practice is associated with pain, suffering and damage to the affected animals. Breeding for a shorter tail in long-tailed sheep breeds could offer one of the alternatives. This study aimed to analyze the natural tail length variation in the most common German Merino variety, and to identify possible causal alleles for the short tail phenotype segregating within a typical long-tailed breed.

Results

Haplotype-based mapping in 362 genotyped (Illumina OvineSNP50) and phenotyped Merinolandschaf lambs resulted in a genome-wide significant mapping at position 37,111,462 bp on sheep chromosome 11 and on chromosome 2 at position

94,538,115 bp (Oar_v4.0). Targeted capture sequencing of these regions in 48 selected sheep and comparative analyses of WGS data of various long and short-tailed sheep breeds as well as wild sheep subspecies identified a SNP and a SINE element as the promising candidates. The PCR genotyping of these candidates revealed complete linkage of both the candidate variants. The SINE element is located in the promotor region of *HOXB13*, while the SNP was located in the first exon of *HOXB13* and predicted to result in a nonsynonymous mutation.

Conclusions

Our approach successfully identified *HOXB13* as candidate genes and the likely causal variants for tail length segregating within a typical long-tailed Merino breed. This would enable more precise breeding towards shorter tails, improve animal welfare by amplification of ancestral alleles and contribute to a better understanding of differential embryonic development.

Keywords: sheep, lambs, tail length, docking, animal welfare, mapping study, *HOXB13*

Background

Sedentary human communities began sheep management as early as 10,000-11,000 BP in an area stretching from central Anatolia to northwestern Iran [1]. It is proposed that the Asiatic mouflon (*Ovis orientalis*), which was common in the same area, was the wild ancestor. The Asiatic mouflon, like other wild sheep subspecies, is a short-tailed hair sheep. Accordingly, the first domesticated sheep were also short-tailed hair sheep, kept mainly for their meat [2]. The systematic production and processing of wool did not occur until several millennia later, leading to the "Secondary Product Revolution" [3] and the worldwide spread of wool sheep. Long-term selection for fine wool fibers culminated in the economically most important and widespread sheep breed, the Merino. All Merinos are characterized by long tails and the common occurrence of fine wool and long tail led to the frequent opinion that these phenotypes are also genetically coupled or the result of the same artificial selector [4]. This assumption could not be proven directly, however, in today's sheep husbandry systems the long woolly tail comes with several problems, e.g. the accumulation of dags in the tail area, which predisposes for flystrike [5]. Therefore, most lambs of long-tailed breeds worldwide are docked shortly after birth [4]. With increasing importance of animal welfare in our society and subsequent restrictions and prohibitions of practices that cause pain and suffering to animals, tail docking has come under scrutiny. In Scandinavia, tail docking without a veterinary indication has already been made illegal [6] and in the Netherlands, exclusions from the docking ban have only been granted for three long-tailed English breeds under the condition of an effective breeding program for shorter tails [7]. In Austria, tail docking in lambs is allowed until an age of 7 days, provided the operation is done by a veterinarian or another qualified person and an analgesic for intra- and post- operative pain-relief is given [8]. The German Animal Welfare Act currently still allows tail docking without anesthesia for lambs under eight days of age, but future amendments will probably seek to eliminate exceptions to the amputation ban [9].

These developments clearly show that a long-term non-invasive alternative for the painful practice of tail docking is urgently needed. Here, a genetic solution offers itself. A high ethical acceptance of genetic breeding for a shorter tail could be expected as all wild sheep subspecies and thus also the ancestor of today's domestic sheep have naturally short tails [10,11]. Therefore, this breeding could be seen as a "back to the roots" program.

The genetic basis for shorter tail breeding efforts is provided by the medium to high heritability of tail length in different sheep breeds, e.g. 0.58 in Merinos [12] or 0.77 in Finnish landrace sires [13]. James, et al. [14] suggest that the inheritance of tail length in Australian Merino depends on a small number of interacting genes of large effects, in which short tail genes show a possible dominance. The presence of various short-tailed Nordic breeds offers a possibility of genetic reduction of tail length by introgression of the desired genetic variants from short-tailed breeds. Scobie and O'Connell [15] crossed short-tailed Finnsheep with long-tailed Cheviot sheep, and observed that an increased proportion of Finnsheep genes led to a proportional reduction in tail length. However, this option is unpopular with breeders, as crossing is associated with the loss of breed-specific traits and a possible decline in previously achieved breeding progress in important production traits.

As an alternative, breeders in Australia and New Zealand attempted genetic shortening of the tail by phenotypic selection within individual breeds. However, Carter [16] reported for Romney sheep that breeding for the short-tail phenotype possibly reduced the viability of embryos that were homozygous carriers of some putative short-tail alleles. In Merinos, James, et al. [14] observed increased incidences of rear-end defects. Zhi, et al. [17] discovered a c.G334T mutation in the *T* gene in the native Chinese Hulunbuir breed and showed that the T allele leads to the extreme short-tailed phenotype, i.e. tailless animals with exposed anus. To prove the causality of this mutation, they genotyped 120 short-tailed Hulunbuir sheep. The observed frequencies of the genotypes (17 G/G, 103 G/T and no T/T) are consistent with the embryonic lethality due to the T/T genotypes in *T* gene [17]. A comparable association between short tails and embryonic

lethality or malformations has been demonstrated in various breeds of dogs and cats too [18-20]. These undesirable negative side effects discouraged and slowed down active breeding programs against overlong tails in the economically most important wool sheep breeds. Moreover, there have been no successful genetic mapping studies in long-tailed Merino sheep breeds, and the possible relationship between the short tail phenotype and embryonic viability or hind end malformations has never been investigated on a genetic basis in Merinos.

The aim of the present study was therefore:

1. To investigate the phenotypic and additive genetic variance in tail length in the Merinolandschaf, which belongs to the economically most important long-tailed Merino breed group worldwide;
2. To map the position of the major QTL(s) affecting tail length;
3. To detect and confirm causal candidate genes by sequencing and genotyping;
4. To determine the distribution of ancestral and derived alleles in a wide range of domestic sheep breeds with different tail lengths as well as in different wild sheep subspecies;
5. To contribute to the understanding of the relationship between genotype and phenotype during embryonic patterning and early development;
6. To put causal alleles in the evolutionary context of sheep species;

Together these objectives will enable more efficient breeding towards the ancestral phenotype and thus improve animal welfare in sheep production without negative side effects.

Materials and Methods

Animal samples and phenotypes

The entire mapping design of 362 phenotyped and genotyped animals were collected in three phases: (i) 236 Merinolandschaf lambs with very short (104) or long (132) tails were selected

for phenotyping and sampling from 2293 visually inspected lambs on a farm in Lower Bavaria with no custom of tail docking, (ii) 102 random male lambs from the same farm were phenotyped and sampled, i.e. without preselection by visually inspected of tail-length and (iii) 24 Merinolandschaf lambs with short (19) or long (5) tails were selected from 102 visually inspected lambs by the Justus Liebig University of Giessen (JLU) (**Table 1**).

Phenotyping of these 362 lambs was conducted according to the method proposed by Eck, et al. [21]. Although an age of 5 weeks proved to be the optimal time point for phenotyping, we sampled and phenotyped also younger and older lambs in order not to disturb the work processes on the farm. Tail length (TL) was measured with a custom-made wooden board from the anus to the tip of the tail, body weight (BW) with a standard scale, and height at the withers (WH) with a metal measuring device from dog sports from the floor to the highest point of the withers. Furthermore, gender, age, and litter size were recorded. Unfortunately, the age and litter size are only approximately known for randomly sampled 102 animals. To improve haplotype inference, we sampled and genotyped 22 putative fathers of the above lambs. These rams were not phenotyped and contributed only indirectly to the QTL mapping.

All blood samples were taken according to best veterinary practice and under a permit from the Government of Upper Bavaria (permit number: 55.2-1-54-2532.0-47-2016), or the Regional Council of Gießen, Hassia (KTV number: 19 c 20 15 h 02 Gi 19/1 KTV 22/2020).

Genotypes

All 362 phenotyped lambs and 22 sires were genotyped using Illumina's OvineSNP50 BeadChip (Illumina, San Diego, USA) according to the manufacturer's specifications. All physical marker positions were determined on the ovine reference genome assembly Oar_4.0 (https://www.ncbi.nlm.nih.gov/assembly/GCF_000298735.2) and the positions of all markers or sequences in materials, results or discussed below correspond to the Oar_4.0 reference

166 genome unless otherwise stated. The chip contains 54,241 SNPs almost evenly distributed
167 across the genome with an average marker spacing of 50.9 kb [22]. Not all of these 54,241 SNPs
168 were used for mapping. We filtered SNPs according to the following exclusion criteria: (i)
169 unsuccessful genotyping in more than 5 % of the animals, (ii) frequent paternity conflicts in
170 animals with known paternity, (iii) unknown position in the reference genome, (iv) minor allele
171 frequency (MAF) of less than 0.025, and (v) localization on a sex chromosome since the
172 analyses were exclusively carried out on autosomes. As a result, 45,114 markers remained in
173 the marker set for the mapping analyses. Haplotype phasing and imputation were conducted
174 using a Hidden Markov Model (HMM) implemented in *BEAGLE* version 5.0 [23]. To improve the
175 accuracy of haplotyping and imputation, genotype and pedigree information from about 5,100
176 additional animals genotyped with the OvineSNP50 BeadChip but not phenotyped were added
177 to the haplotyping design [24].
178

179 ## Estimation of heritability and mapping

180 First, we tested the heritability of the tail length in the pure Merinolandschaf breed. For this
181 purpose we used the software *GCTA* v1.93.2, which has been extended with GRM, a tool for
182 estimating the genetic relationship matrix and a genomic-relatedness-based restricted
183 maximum-likelihood approach (GREML), to estimate the proportion of variance in our
184 phenotype explained by all SNPs (the SNP-based heritability) [25]. The sex, age, weight, and
185 withers height of the lambs at phenotyping were modeled as fixed effects.
186

187 ### Mixed linear model-based association analysis

188 To map a putative tail length locus, we performed mixed linear model-based association
189 (MLMA) analyses with a leave-one-chromosome-out (LOCO) approach (Model 1) as
190 implemented in the software *GCTA* v1.93.2 [26]. Here we used the following model:

$$\mathbf{y} = \mathbf{X}ß + \mathbf{Z_a a} + \mathbf{Z_u u} + \mathbf{e}$$

where **y** is the vector of tail lengths (cm), **ß** is a vector of fixed effects including the mean, sex, age, body weight (BW) and withers height (WH) at phenotyping, **a** is the vector of the additive effect (fixed) of the candidate SNP to be tested for association, **u** is the vector of polygenic effect (random or accumulated) of all markers, excluding those on the chromosome which contains the candidate SNP and **e** is a vector of residuals. **X**, $\mathbf{Z_a}$ and $\mathbf{Z_u}$ are the incidence matrices for **ß**, **a** and **u**, respectively.

The suggestive significance threshold was set at $P < 1/N$ and the genome-wide significance threshold at $P < 0.05/N$, according to Bonferroni method, N stands for the number of markers [27]. For initial MLMA-analysis we considered 45,114 markers resulting in the suggestive P-value at 2.22×10^{-5} and genome-wide at 1.11×10^{-6}.

A second MLMA (Model 2) analysis included one additional locus, which we detected during our research, as a consequence, we considered 45,115 markers. The suggestive and genome-wide significance threshold remained the same.

Combined linkage disequilibrium and linkage analysis (*cLDLA*)

Parallel with SNP-based association analyses using MLMA, we performed multiple haplotype-based *cLDLA* analyses [28], which have been successfully used for binary and quantitative trait mapping in previous studies [29-32].

To correct for familial relationships and population stratification, unified additive relationships (UARs) were estimated between all animals on a genome-wide level [33]. The inverse of the UAR matrix was then included in the variance component analysis. To account for linkage disequilibrium in the form of local haplotype relationships, the Locus IBD (LocIBD) was estimated according to the method of Meuwissen and Goddard [34] using sliding windows of 40

SNPs. For each window, we estimated LocIBD in the middle, i.e. between SNPs 20 and 21, based on the flanking marker haplotypes. Following the method for additive genetic relationship matrices ($\mathbf{G_{RM}}$) by Lee and Van der Werf [35], the matrix of LocIBD-values was converted into a diplotype relationship matrix ($\mathbf{D_{RM}}$).

Variance component analyses were carried out with the program *ASREML* [36] according to the method of Meuwissen, et al. [28]. *ASREML* estimated the maximum likelihood, variance components, and fixed and random effects simultaneously by considering the genome-wide UAR as well as the locus-specific ($\mathbf{D_{RM}}$) relationships matrices in the following mixed linear model:

$$\mathbf{y} = \mathbf{X\beta} + \mathbf{Z_1u} + \mathbf{Z_2q} + \mathbf{e}$$

where $\mathbf{y}$ is again the vector of tail lengths and $\boldsymbol{\beta}$ is the vector of fixed effects (BW in kg, WH in cm, sex, age, and the overall mean μ; BW and WH data were both standardized and centered). The vector $\mathbf{u}$ is the vector of random polygenic effects (with $\mathbf{u}\sim N(0, \mathbf{G}\sigma_u^2)$ where $\mathbf{G}$ represents the matrix of genome-wide IBD estimations), $\mathbf{q}$ is the vector of random additive-genetic QTL effects (with $\mathbf{q}\sim N(0,\mathbf{D_{RMp}}\sigma_q^2)$ where $\mathbf{D_{RMp}}$ is the diplotype relationship matrix at position p of a supposed QTL), and $\mathbf{e}$ is the vector of random residual effects (with $\mathbf{e}\sim N(0, \mathbf{I}\sigma_e^2)$, where $\mathbf{I}$ is an identity matrix). It is assumed that $\mathbf{u}$, $\mathbf{q}$ and $\mathbf{e}$ are not correlated. $\mathbf{X}$, $\mathbf{Z_1}$, $\mathbf{Z_2}$ are incidence matrices linking the observed values with the fixed and random QTL effects.

The variance components and likelihood estimated with *ASREML* were then used in a likelihood ratio test statistic (*LRT*). The *LRT* values follow a χ^2 distribution with one degree of freedom [37] and were calculated as:

$$LRT_p = -2 \times (\log(L_0) - \log(L_{1p}))$$

where $\log(L_0)$ is the logarithm of the likelihood estimated by *ASREML* for the model without and $\log(L_{1p})$ with QTL effects at the center of the window p.

To obtain a significance threshold, a Bonferroni correction was carried out to account for multiple testing due to the 40-SNP sliding windows [38]. This resulted in a corrected *P*-value of

243 $< 4.44 \times 10^{-5}$ (i.e., 0.05/1127 where 1127 is the number of nonoverlapping 40 SNP windows)
244 and a corresponding *LRT* value with genome-wide significance is equal to 16.67.
245 In addition to Model 3 described above, we performed two further genome-wide cLDLA
246 analyses, with both analyses using candidate locus genotypes for the same set of animals. Model
247 4 contains only one additional locus and is therefore comparable to Model 2 of MLMA. In
248 Model 5, the genotypes of the same candidate locus are considered as a fixed effect, i.e. **β** is the
249 vector of μ, sex, age, BW, WH, and candidate locus effects. A comprehensive overview of the
250 different models is provided in **Table 2**. For all maxima of the LRT curve (*LRT*max) that
251 exceeded the genome-wide significance threshold, the 2-LOD (logarithm of the odds) criterion
252 was used to determine the associated confidence intervals [39]. Closely located LRT peaks were
253 assumed to belong to the same QTL as described by Müller et al [32].
254
255 The results of the association analyses were presented as Manhatten plots produced by the *R*
256 package *QQMAN* [40].
257

258 ## Annotation of gene content and gene set enrichment analysis

259 The confidence intervals of the *LRT*max were compared with a map of annotated genes in the
260 UCSC Genome Browser Oar_v4.0/oviAri4 Assembly [41,42] using the "RefSeq Genes" track. We
261 refer to the Ensembl database of (Oar_v3.1) [43], the Mus musculus Assembly (GRCm39) [44], and
262 the Homo sapiens Assembly (GRCh38.p13) [45] from NCBI [46] as well to consider genes
263 encompassing the confidence intervals. Next, gene set enrichment analyses were carried out
264 with the software *ENRICHR* (Ontologies, MGI Mammalian Phenotype Level 4 2019) [47,48].
265

DNA extraction, sequencing and analysis of the sequences

Genomic regions where the LRT curve reached a maximum value above the genome-wide significance threshold were sequenced using targeted capture sequencing on 48 selected lambs. To minimize the risk of missing some causal variations that are close but outside the confidence intervals, we increased the candidate regions on both sides by about 300 kb. This resulted in the captured regions on OAR2 from 93.200.000 to 96.700.000bp and on OAR11 from 36.600.000 to 37.900.000 bp. Genomic DNA was extracted from the blood samples using the ReliaPrep™ Blood gDNA Miniprep System.

Whole-Genome sequencing libraries were prepared from 250 ng of genomic DNA by tagmentation with the NexteraFlex kit from Illumina. Subsequently, the libraries were dual-barcoded and amplified by PCR, purified with SPRI beads and pooled in equimolar amounts. The pooled libraries were enriched for the target regions by hybridization to an Agilent capture array with 244k oligo spots. The oligo probes were selected from the repeat-masked DNA sequence as all possible 60mers that do not overlap with repeat-masked bases and that are staggered in 15 nt tiling steps concerning their neighbors. After 65 hours of hybridization in the presence of cot-I sheep DNA and adapter blocking oligos at 65°C the capture array was washed and the captured library molecules were eluted at 95°C for 10 min in a volume of 500 µl DNA-grade water. The enriched libraries were then amplified by PCR, analyzed on the Bioanalyzer and sequenced in 2*110 bp paired-end mode on a P2 flowcell of a NextSeq1000 sequencer from Illumina.

SICKLE [49] was used to trim the adaptors and filter low-quality sequences of the raw reads in the FASTQ files. With *FASTQC* [50], we assessed the quality parameters of the filtered sequencing data. The filtered reads were mapped to the sheep reference genome OAR_v4.0 using the default parameters of *BWA-MEM* [51] alignment tool. To convert the SAM files into coordinate sorted BAM files and to remove the duplicated reads, *SAMTOOLS* [52] and *PICARD* [53] were used. Base quality recalibration and indel realignment were done with *GATK* [54]. Variant calling was

292 performed with *BCFTOOLS* (mpileup) [55] for SNPs. To detect indels and structural variants (SV)
293 we used *SMOOVE* (*LUMPY*)[56] and *DELLY* [57] with default parameters.
294 To ensure that we do not miss any candidate variant we performed a visual examination of the
295 captured regions using *JBROWSE* [58], focusing on the region our candidate gene is located. We
296 also examined the genetic variance in open source WGS of three sheep groups: 1) long-tailed
297 domestic sheep, 2) short-tailed domestic sheep and 3) short-tailed Asiatic mouflon. **Table 3**
298 shows the examined breeds/species including the Run-numbers and Biosample IDs.
299

300 Validation of candidate SNP using PCR

301 For one detected candidate SNP we performed genotyping by PCR-RFLP and electrophoresis
302 on a 2% agarose gel on all 362 sampled lambs and there 17 confirmed fathers. The PCR primer
303 sequences designed by *PRIMER3* [59] were TTTAAAACGCTTTGGATT (Forward, Left Primer)
304 and CACTCGGCAGGAGTAGTA (Reverse, Right Primer). The used restriction enzyme was
305 *BsrI*. It recognizes the mutant sequence TGAC/CN, where the G is the variable base and the "/"
306 presents the site where cutting is performed. DNA amplification was performed with 35 cycles.
307 The total reaction mixture was 15.0 µl containing 3.0 µl 5X buffer, 1.5 µl dNTPs (10mM), 0.6
308 µl of 10 µM Forward and Reverse Primer respectively, 1.0 µl DNA (15 ng/µl), 0.07 µl
309 GoTaq®G2 DNA Polymerase (Promega, Madison, Wisconsin, USA) and distilled water.
310 We used 1.5 U of the enzyme *BsrI*, 3.0 µl DNA (PCR product), 2 µl Cut Smart Buffer, and
311 distilled water for a total reaction volume of 20 µl. The reaction mixture was afterward
312 incubated for 3 h at 65 °C. In the final step, we separated the DNA fragments by size and
313 visualized them by GelRed™-stained agarose gel electrophoresis. Only sequences harboring
314 the derived allele (SNP G) were cut, the two resulting fragments had a length of 120 bp and 259
315 bp. The sequence with the ancestral allele (SNP C) retained its length of 379 bp.

Validation of candidate insertion using PCR and Sanger sequencing

We also performed genotyping by PCR and electrophoresis on a 2% agarose gel on the same 379 sampled sheep for one detected causal candidate insertion. Multiple PCR primer sequences designed by *PRIMER3* [59] were tested (Supplementary Table S1), those that worked best are TTTATGAGCTTCTCTCCGCCA (Forward, Left Primer) and CACTCGGCAGGAGTAGTA (Reverse, Right Primer). DNA amplification was performed with 35 cycles. The total reaction mixture was 25.0 µl containing 5.0 µl 5X buffer, 2.5 µl dNTPs (10mM), 1 µl of 10 µM Forward and Reverse Primer respectively, 1.0 µl DNA (15 ng/µl), 0.07 µl GoTaq®G2 DNA Polymerase (Promega, Madison, Wisconsin, USA) and distilled water. In the final step, we separated the amplicons by size and visualized them by GelRed™-stained agarose gel electrophoresis.

Two lambs, which are homozygous for the SV, one lamb, which is homozygous for the ancestral allele and two heterozygous lambs were resequenced using Sanger sequencing with the above mentioned best working Primers. The amplicons were sequenced using the cycle sequencing technology (dideoxy chain termination / cycle sequencing) on ABI 3730XL sequencing machines (Eurofins Genomics, Germany). The sequenced data were analyzed using *SNAPGENE* software (from Insightful Science; available at https://www.snapgene.com/).

Results

Initial mixed linear model association analysis

The *GCTA-GREML* analysis revealed SNP-based heritability of 0.992 (standard error of 0.12), meaning that a very high proportion of the tail length variance in Merinolandschaf breed is explained by genome-wide SNP markers. Despite very high heritability, i.e., close to 1, the initial association analysis (MLMA Model 1) revealed no genome-wide significant association between any SNPs and tail length. Even the four most significant SNPs (**Figure *1*a**) remain below the suggestive significance threshold of $P = 2.22 \times 10^{-5}$.

Initial combined linkage disequilibrium and linkage analysis

The haplotype-based cLDLA mapping (cLDLA Model 3) resulted in two genome-wide significant QTLs associated with tail length in Merinolandschaf (**Figure *1*c**). The most prominent and narrow peak is on the sheep chromosome 11 (OAR11) at position 37,111,462 bp with *LRTmax* = 29.460 corresponding to $P = 5.71*10^{-8}$ (Bonferoni corrected: $P = 6.43*10^{-5}$). The second genome-wide significant QTL affecting tail length was mapped to the chromosome 2 at position 94,538,115 bp with *LRTmax* = 19.356 corresponding to $P = 1.08*10^{-5}$ (Bonferoni corrected: $P = 1.22*10^{-2}$).

Applying the 2-LOD criterion, the corresponding confidence interval was set for the *LRTmax* on OAR11 between positions 37,000,925 bp and 37,521,490 bp and for the maximum value on OAR2 between positions 93,441,900 bp and 96,402,884 bp. These intervals were then considered in the UCSC Genome Browser Oar_v4.0/oviAri4 Assembly, which resulted in the list of genes summarized in **Table *4*** and **Table *5***. The list of positional candidates also includes obvious functional candidates from the sheep homeobox B gene cluster (Chr11:37,290,203-37,460,240) with *HOXB13* (37,290,203-37,292,513) as the closest and most prominent candidate, lying only 179-Kb proximal to the *LRTmax*.

Additional chromosome-wide significant peaks were observed on OAR2, OAR3, OAR10, OAR14, and OAR17. However, these peaks show *LRT* values far below the genome-wide significance and thus, were not investigated further.

Estimation of QTL effects and selection of animals for capture sequencing

In the previous step of cLDLA, we used *ASReml* to estimate variance components, fixed and random effects affecting tail length in Merinolandschaf breed. Here, we analyzed in more detail the estimated effects at loci with the most significant association, i.e. at loci showing *LRTmax*

values. We sorted all 362 lambs according to the random additive genetic QTL effects (vector **q**) estimated at *LRTmax*. Together with the QTL effects, we simultaneously considered all input (**y**, sex, age, WH, BW, maternal and paternal haplotypes at 40-SNP window with *LRTmax* in interval between SNP 20 and 21) and output data (**u**, **ß** and **e**) that contributed to *LRTmax*. Visual inspection of this table allowed us to select 48 lambs (half with the most negative and half with the most positive additive genetic QTL effects) for targeted capture sequencing. Supplementary Figure S1 and S2 show the distribution of the sequenced lambs regarding tail length and diplotype effects on OAR2 and OAR11

A regression analysis performed with the function *lm* in *R* [60] estimated the adjusted coefficient of determination of R^2=0.58 for the *LRTmax* on OAR11 and only R^2=0.15 for the *LRTmax* on OAR02 when using tail length as the dependent and diplotype effect as the independent variable. Adding, age, sex, BW and WH as additional independent variables yield R^2=0.78 for QTL on OAR11 and R^2=0.45 for QTL on OAR02 (Supplementary Table S2 and S3). According to the shape of the LRT curve, the significance of the mapping and the coefficient of determination, the haplotypes associated with the putative causative alleles are more distinct in QTL on OAR11 than on OAR02. However, the selection of 48 lambs for capture sequencing represents a trade-off between the two QTLs, with the choice for OAR11 being more decisive. The selected lambs could be divided into two groups: 23 long-tailed with positive QTL effect and 25 short-tailed lambs with negative QTL effect on OAR11. Sorting the same lambs by QTL effects on OAR2 changes the order within the group and results in 3 individuals from the long-tailed group and 4 individuals from the short-tailed group moving to the other group.

Capture sequencing of 48 lambs and detection of candidate mutations

Capture Sequencing was carried out at a mean depth between 0.41 and 2.45 on the target region of OAR2 and between 1.01 and 2.39 on the target region of OAR11. This coverage is much lower than intended and most possibly caused by competition with WGS performed on the same

sequencing lane. However, applying default settings of BCFTOOLS MPILEUP on the individual samples, we detected 27,256 and 74,485 SNPs respectively on OAR11 and OAR02. Next, we sought to identify variants showing significant differences in frequency between short-tailed and long-tailed groups. Interestingly, of all the detected genomic variations, only one SNP satisfied the frequency-based criterion; this SNP (C→G) was located on OAR11 at the position of 37,290,361. The visual examination using *JBROWSE* confirmed the base substitution (*rs413316737*) as a nonsynonymous point mutation within the first exon of *HOXB13* (relative position 23). The point mutation results in a p.(Thr8Ser) substitution. All sequenced Merino lambs from the long-tailed group are homozygous for this missense variant (G/G). In the short-tailed group, 4 lambs are homozygous G/G, 6 are heterozygous C/G and 15 are homozygous C/C on that position. The Ensembl Variant Effect Predictor [61] predicted a SIFT score of 0.54 and classified the mutation as so-called "*Tolerated*" missense variant.

In the next step, protein BLAST [62] was used to align the amino acid sequence of the mutant HOXB13 protein against the amino acid sequence of wild-type HOXB13 protein of different mammals including all the extant wild sheep species (**Table 3**). This cross-species alignment (**Figure *2***) revealed that the amino acid at which the variant discovered here occurred is conserved. In addition, 5 downstream amino acids are also conserved among here aligned species.

By comparing the allele frequency in long-tailed and short-tailed sheep in multiple breeds, we observed that the above-mentioned derived allele G occurs more frequently in long-tailed sheep breeds (Supplementary Table S4). Further, at this position, we only observed the ancestral allele in Urial, Argali, Snow sheep, Dall sheep, Canadensis and two ancient (~8,000 years) sheep genomes [63]. On the other side out of 16 investigated Asiatic mouflon 3 were heterozygous C/G

and 2 homozygous G/G for the point mutation. However, it is worth mentioning here that one Asiatic mouflon (G/G) and the two ancient WGS have low coverage (**Table 3**) at this locus.

To investigate the pattern of structural variations (SVs), we increased the sequencing coverage of both the groups by pooling the raw reads of their respective samples. Further, we identified SVs in the targeted region (between 36,600,000 and 37,900,000 bp) of OAR11 from these data by using the three different approaches: *SMOOVE*, *DELLY* and visual examination using *JBROWSE*. Using the strict threshold criteria, i.e. SV not present in a pooled sample of short tail sheep but present in a pooled sample of long tail sheep, we identified 27 and 32 SVs from *SMOOVE* and *DELLY* approaches, respectively. However, it is noteworthy that our captured sequencing had highly non-uniform and relatively low coverage, therefore, these approaches might have missed many true positive and included high number of false positives. In fact, our visual examination of these regions also indicated so (Supplementary Figure S3).

Interestingly, window-by-window visual examination of the targeted region in *JBROWSE* revealed two distinct clusters of reads showing soft-clipped (**Figure 3a**) just about ~130 bp upstream of the candidate SNP. Both these clusters were arranged next to each other; while one cluster was present in all the sequenced animals, indicating either assembly error or assembly-specific variant as the likely cause. Another cluster of soft-clipped reads had distinct frequency distribution between the groups of short-tailed and long-tailed reads. At position 37,290,229 on OAR11, the long-tailed group showed 34 of the 35 reads mapped as soft-clipped, while the short-tailed group showed 13 of the 54 reads as soft-clipped.

We also observed a significant difference in the frequency of the clipped reads around this position between the WGS data of short and long-tailed sheep that were downloaded from NCBI SRA (**Table 3**). Therefore, in the next step, we aligned the pooled reads of the short-

tailed and the long-tailed group and the WGS data of NCBI SRA against the latest sheep assembly (ARS-UI_Ramb_v2.0). Visual examination of the region upstream of the first exon of *HOXB13* gene on OAR11 revealed only one cluster of soft-clipped reads at positions 37,524,996 (**Figure 3b**) indicating that another cluster which was identified in the mapping against Oar 4.0 assembly was due to missing sequences of about 40 bp in Oar 4.0 assembly. Interestingly, we observed that a very high number of soft-clipped reads in this cluster had supplementary alignment on OAR5. Further, on OAR11 at the breakpoint, we also observed discordant alignment (overlapped) between forward and reverse reads. Based on the presence of the soft-clipped reads and discordant alignment, we suspected the presence of insertion or translocation. While we were investigating this region on ARS-UI_Ramb_v2.0 assembly, we came across a pre-print by Li, et al. [64]; they reported insertion in the same region using the graph-assembly based method on the Pac-bio sequencing data of 13 different sheep breeds.

To investigate the soft-clipped regions further, we carried out Sanger sequencing of 5 samples, based on the previously described candidate SNPs. The analysis of the Sanger sequencing data (**Figure 3c**) and subsequent alignment against OAR11 in ARS-UI_Ramb_v2.0 using *BLAST* identified the SV as an insertion of 167 bp. Interestingly, we further observed that this sequence is flanked by 14 bp of direct repeats (CTGCCAGCGATTTA) on both sides. Therefore, we hypothesized that this insertion could be a part of SINE repeat family. Next, we searched for this sequence in DFAM repeat database and identified it as belonging to OviAri-1.113 SINE family.

Genotyping of the most plausible candidates in 362 lambs and remapping of tail length

To confirm the association between the detected variants and tail length, we performed genotyping of these two candidates in the entire mapping population and used genotypes in the

GWAS and cLDLA Model 2, 4 and 5 (**Table 2**). The PCR-genotyping of the candidate SNP resulted in 220 G/G, 118 C/G and 24 C/C lambs. The PCR-genotyping of the 132 bp upstream candidate insertion of 167 bp showed an identical distribution of genotypes over entire mapping population, i.e. insertion occurred in all haplotypes harboring the base G and never in haplotypes harboring C on the position 37.209.361. Due to the complete linkage between the insertion and the missense SNP, both candidates are considered synchronously and equally in Model 2 (MLMA) and Models 4 and 5 (cLDLA). The distribution of alleles in wild sheep subspecies and domestic sheep allow us to infer ancestral and derived alleles at both candidate loci. The absence of insertion and base C at c.C23G SNP of *HOXB13* are ancestral while 167bp insertion and base G are referred to derived alleles.

All lambs homozygous for ancestral alleles could be classified as short-tailed with mean tail-length 24.1 cm (±1.34) and mean QTL effect -2.92 cm (±0.71). On the other side lambs homozygous for derived alleles classified as long-tailed as well as short-tailed. Consequently, lambs with derived homozygous genotype show higher average tail length 31.5 cm and 4.15 times higher standard deviation of tail length (±5.56). Lambs with heterozygous genotype show average tail length of 25.7 and 2.73 times higher standard deviation (±3.66). The **Table 6** summarizes phenotype, QTL and polygenic effects of candidate insertion and SNP that are in population-wide linkage disequilibrium.

***MLMA* and *cLDLA* including candidate variants as markers**

To investigate the impact of derived alleles on the results of the SNP-based association analysis and the haplotype-based mapping we considered candidate locus as an additional marker located on Chr11:37,290,361 (see Model 2 and 4 **Table 2**). Thereby, only the number of considered markers increases by one compared to the original analysis, while the other input data, as well as the parameters and the model, do not change. This minimal change in the input data led to enormous changes in the results of the association analysis and limited changes in

the results of the haplotype-based mapping. *MLMA* Model 2 confirmed the candidate causal locus as a uniquely genome-wide significant (P = 6.2 *10^{-12}) locus, while *cLDLA* revealed a slightly altered significance (*LRTmax*=29.112) at the slightly altered position 37,311,842 bp. However, in the initial mapping *LRTmax* was 179 Kb away from *HOXB13*, and the Model 4 of *cLDLA* placed *LRTmax* between *HOXB13* and *HOXB9* (**Fehler! Verweisquelle konnte nicht gefunden werden.**). Therefore, the distance between *LRTmax* and the candidate gene *HOXB13* decreased from 179 Kb to 19 Kb, and thus *HOXB13* became the closest gene to *LRTmax*.

Variance components, *MLMA* and *cLDLA* including candidates as fixed effect

The above results point to *rs413316737* and/or the insertion as plausible candidates for causal variations. The mixed linear model (MLMA or cLDLA) allows us to model important causal candidates and thus improve the mapping of residual variance (if present) in the mapping population. To investigate the presence of additional loci affecting tail length in long-tailed Merino sheep, we modelled the genotypes at the candidate insertion and SNP as fixed effects, i.e. lambs with homozygous ancestral genotype were classified as class 1, heterozygous as class 2 and homozygous derived as class 3, while the other input data, parameters and model did not change. We first estimated the SNP-based heritability of tail length after correcting for the most significant causal candidates. The heritability decreased from h^2=0.992 to 0.898. This indicates still high proportion of the additive genetic variance in phenotyping variance corrected for the most plausible candidate mutations in *HOXB13*. However, as shown in **Figure 1d**, the cLDLA is unable to highlight additional candidates, although a relatively high proportion of additive genetic variance is still present in the mapping population studied here (h^2=0.898). As expected from the true candidate, the mapping signal on OAR11 disappeared completely (**Figure 1dFigure *2***). Moreover, the LRT value at the peak on OAR02 decreased from 19.356 to 14.476

514 and marginally changed his position from 94.538.115 bp to 94.345.619 bp. With this change, a
515 possible QTL on OAR02 loses its significance.
516

517 Discussion

518 The present study aimed to identify the genes or variants responsible for the natural variability
519 of tail length in the Merinolandschaf breed. The results presented here suggest that the
520 inheritance of tail length depends largely on additive genetic variance almost without
521 environment effects (h^2 =0.992). Despite the relatively small number (362) of phenotyped and
522 genotyped animals, heritability was estimated with a relatively low standard error (SE=0.12).
523 According to Visscher et al [65], the SE depended only on the sample size and became below 0.1
524 by using more than ~3000 independent individuals.
525 The GWAS (MLMA), i.e. the standard method for mapping loci associated with complex traits
526 and diseases, showed no significant and even no suggestive association in our design with 362
527 animals and 45,114 markers. Typically, GWAS [65] uses several hundred thousand markers in
528 large mapping designs. Therefore, the solution would be to enlarge the sample size and
529 genotype this enlarged mapping design with high marker density (e.g. OvineHD). However, in
530 studies such as this, where phenotypes are not routinely collected, the number of phenotyped
531 animals may be limited or can only be expanded at great expense. On the other hand, the number
532 of markers can also be a limiting factor in many species, e.g. there is only 50K chip for domestic
533 goats. The alternative solution could be to apply a mapping method that uses more information
534 from the current design. Due to time and cost constraints, we opted for haplotype-based
535 mapping and obtained a highly significant (P = 5.71*10^{-8}) and fine mapped QTL on OAR11
536 (CI 37,000,925 - 37,521,490 Mb) as well as another genome-wide significant result (P =
537 1.08*10^{-5} with less sharp mapping (OAR02, CI 93,441,900 - 96,402,884 Mb).
538

Previous research on tail length in domesticated animals, including sheep, mainly pointed to the *T* gene, also known as the brachyuria gene, as a candidate causal gene. In Hulunbuir short-tailed sheep, a *c.G334T* mutation in *T* gene is the main cause of the extreme short-tail phenotype [17]. Mice that are heterozygous for mutations in the *T* gene have a short tail and homozygous embryos die in the middle of the gestation [66-68]. In Manx cats, the short-tailed phenotype is caused by naturally occurring mutations in *T* gene [19], in particular by three 1-bp deletions. The *T* gene has also been associated with the short-tailed phenotype in various dog breeds [18,69,70]. Additionally, *ANKRD11*, *ACVR2B* and *SFRP2* were detected as plausible candidate genes that could contribute to the reduction in tail length in particular dog breeds [69] and the somite segmentation-related gene *HES7* [71] in Asian domestic cats.

In this study we could not detect any increase in the LRT curve in the *T* gene region (OAR8: 87,717,306–87,727,483 bp). Furthermore, neither *ANKRD11* (OAR14: 13,810,611–13,882,911 bp), *ACVR2B* (OAR19: 11,794,562–11,802,479 bp) or *SFRP2* (OAR17: 3,727,698–3,736,241 bp) showed a significant increase in the LRT value. *HES7* is located on OAR11 (27,284,897-27,287,414 bp) but is 10 Mb away from the QTL confidence interval and was therefore not considered as a candidate gene for tail length in the Merinolandschaf breed. The confidence interval on OAR11 includes complete ovine *HOXB* cluster and additional seven genes (**Table *4***). Among these genes, a potential influence on tail length could be predicted for *HOXB6*, *HOXB8* and *HOXB13*. Here, *HOXB13* is the gene closest to the maximum *LRT* value and a corresponding literature search (see Diaz-Cuadros, et al. [72] for a review) indicates this gene as the most likely gene causing the large effect in our design. The literature search for plausible candidates for genes at OAR02 (**Table *5***) yielded hardly any useful results. We tried to improve our search with MGI Mammalian Phenotype level 4 (MMP4) ontology, a method for classifying and organizing phenotypic information related to mammalian species (66). After correction for multiple testing (adjusted $P < 0.05$), 29 ontologies were significantly enriched, but we see no plausible link to tail length.

565 To select the most suitable lambs for capture sequencing of confidence intervals of QTLs on
566 OAR11 and OAR02 we mutually considered haplotypes, phenotypes, fixed effects and random
567 effects at *LRTmax* of both regions. Again, the visual inspections, as well as linear regression
568 analyses, confirmed QTL on OAR02 as inconclusive. This is evident from adjusted $R^2 = 0.58$
569 and only 0.15 for tail length fitted to QTL of OAR11 and OAR02, respectively.
570
571 Consistent with the clues in favor of OAR11 discussed above, capture sequencing revealed one
572 plausible point mutation and one SINE insertion in the QTL region. All Merinolandschaf lambs
573 and their fathers show a complete linkage disequilibrium between these two variants. This is
574 not surprising because these mutations are only 132 base pairs away from each other, and
575 recombination in such a short segment should be extremely rare. We further investigated this
576 linkage in some typical long-tailed and short-tailed breeds (**Table 3**). The linkage was
577 confirmed for long-tailed White Swiss Alpine and Rambouillet breeds but we observed the
578 occurrence of the missense mutation without the insertion in some individuals of short-tailed
579 domestic sheep breeds as well as in five Asiatic Mouflons (**Table 3**). Our analyses of the WGS
580 data (**Table 3**) and amino acid sequence alignment (**Figure 2**) identifies allele C to be ancestral.
581 Therefore, allele G is a derived but relatively ancient allele that segregates in *Ovis gmelini* and
582 *Ovis aries*. The 167 bp insertion in the promotor region is also derived but more recent and
583 segregates exclusively in domestic sheep and predominantly in long-tailed sheep breeds. This
584 insertion occurred in the haplotype with the older missense allele G and both derived alleles
585 segregate as a block. So, we did not observe the insertion without allele G, but we did observe
586 the older allele G without insertion. The presence of the insertion in long-tailed sheep breeds
587 and its location in the promotor region of *HOXB13* increases the probability of insertion as a
588 causative variant for the long tail phenotype. Most likely because of its location the insertion
589 modulates the promoter activity of *HOXB13* and leads to a longer tail by reducing the
590 expression of *HOXB13* gene. Indeed, a recent study by Li, et al. [64] also detected an insertion of

169 bp close to the 5' UTR of *HOXB13* at position 37,525,005 (ARS-UI_Ramb_v2.0) using the graph-assembly based method on the Pac-bio sequencing data of 13 different sheep breeds including Merino. Therefore, it is likely this study and Li, et al. [64] both identified the same insertion. The small differences in length and position of this insertion can be attributed to sequencing error due to the presence of long homopolymer of "T" base in the identified SINE repeat element.

Interestingly, the missense mutation (*rs413316737*) in the first exon of *HOXB13* (37,290,361 C→G) is included on the OvineHD array as SNP marker *oar3_OAR11_37337253*. This offers the possibility to check the allele distribution in available open source genotypes (Supplementary Table S4). It is noteworthy, that top-allele G of *oar3_OAR11_37337253* correspond to ancestral C in the coding sequence of the *HOXB13*. Genotyping of the candidate SNP and insertion throughout the mapping design provides the opportunity to test the efficiency of GWAS and cLDLA with the candidates as a marker and as a fixed effect. The inclusion of the candidates as a marker supports very strong association (i.e. $P = 6.2 * 10^{-12}$) or identity of the *rs413316737* and/or insertion with the causative locus. Additionally, it demonstrates the power of GWAS when the design includes causal variants or markers with population-wide LD. On the other hand, the inclusion of candidates as markers in haplotype-based mapping leads only to partial change, i.e. the mapping significance remains about the same, but the mapping peak is 9-times closer to the most plausible candidate gene. Even more conclusive is the impact of these mutations as a fixed effect in the model, because the correction for the true causal variant should cancel out the LRT peak on OAR11, and if this explains a full additive genetic variance, the heritability should also be reduced towards zero. Indeed, this model erase the LRT peak on OAR11 (**Figure 1d**) but the heritability remains relatively high (0.898). We thus gathered further evidence pointing to a missense mutation in the first exon of *HOXB13* and/or a structural variation in the promotor region of *HOXB13* as plausible causal mutations

617 but also confirmed the presence of other, yet unknown causal variants that explain a large part
618 of the phenotypic variance.
619 The *HOXB13* belongs to the family of homeobox genes, which were first described in
620 *Drosophila melanogaster* [73]. This gene codes for transcription factors and play an important
621 role in structuring the body plan during embryogenesis (reviewed by Diaz-Cuadros, et al. [72]).
622 In mammals, there are 39 *Hox* genes organized in four clusters and 13 paralogous groups [74].
623 There is functional redundancy among the paralogous *Hox* genes [75] and the paralog alleles can
624 compensate for each other to a certain degree [76]. Therefore, the loss of function of one *Hox* gene
625 from a cluster is usually compensated by the functionality of an intact paralogue and only the
626 loss of function of several paralogs results in more severe consequences in axial structuring [74].
627 There is indirect evidence that *HOXB6* [77] and *HOXB8* [78] may influence tail length and
628 embryonic viability. However, capture sequencing finds no genetic variants associated with tail
629 length in any of these two candidate genes. Therefore, we do not discuss these positional
630 candidates further.
631 As vertebrate embryos develop progressively from head to tail, the HOX13 paralogous group
632 has been proposed to control axis termination [72], which is mainly achieved through regulation
633 of proliferation and apoptosis activity in the posterior embryonic regions [79]. In mice, loss-of-
634 function mutations in *Hoxb13* lead to overgrowth of the spinal cord and caudal vertebrae in
635 homozygous mice. These animals consequently show longer and thicker tails while viability
636 and fertility remain unaffected [79]. Premature expression of genes of the *Hox13* paralogous
637 group, on the other hand, negatively influences the extension of the caudal axis and results in a
638 truncated phenotype [78]. Among all candidate genes from the *Hox* family, *HOXB13* is thus our
639 best functional candidate gene. Moreover, Li, et al. [64] used previously published RNA-Seq data
640 of sheep colon, performed a luciferase reporter assays and indicated an association of lower
641 expression of *HOXB13* with insertion in its promotor region. This is in the line with above
642 findings in mice. However, due to complete linkage, we cannot exclude the cooperative

643 causality of the insertion and missense mutation in the exon 1. The *HOXB13* is expressed in the
644 prostate of adult humans and is intensively studied as a candidate biomarker for the prognosis
645 of prostate cancer (see Ouhtit, et al. [80] for review). These studies show that missense mutations
646 in the coding sequence of *HOXB13* can change the affinity [81] or half-life [82] of heterodimer
647 between HOXB13 and e.g. MEIS1 proteins. However, it was not within the scope of this study
648 to investigate the affinity between different transcription factors in growing sheep embryos or
649 cell lines. It is well known that the SINE insertion alone can alter gene expression in multiple
650 ways [83], but we propose to test the hypothesis of a possible causality of the combination of
651 altered expression and altered amino acid sequence.
652
653 As already introduced, attempts were made in 1970s and 1990s to breed short-tailed Romney
654 [16] and Merino [11,14] sheep. These attempts failed due to evidence of reduced viability of
655 presumably homozygous short-tailed Romney embryos and by increased incidences of rear-end
656 defects in short-tailed Merinos. However, these observations contradict the fact that the short
657 tail is the ancestral trait and that old Nordic short-tailed breeds like Romanov and Finnsheep
658 are very viable and highly fertile. Therefore, we assume that these early experiments were not
659 carried out with animals that had shorter tails due to ancestral genetic variants, but due to some
660 recent deleterious variants. James et al [14] wrote that the tail lengths of the four sires measured
661 before mating were all less than 5 cm. This is very short for an adult ram, even much shorter
662 than the tail of short-tailed adult Romanov rams (~20 cm). Also, Romney sheep used for
663 experimental mating by Carter [16] were described as “tailless”. Therefore, short or tailless
664 phenotypes described in initial sheep breeding attempts [14,16] are comparable with deleterious
665 mutations described for certain dog, and cat breeds [18-20,69,70] rather than to some ancestral alleles.
666 In this study detected causal candidates for short tails are highly frequent or fixed in some very
667 viable and highly fertile breeds (e.g. Finnsheep, Romanov, Dalapaels, Soay, Supplementary

668 TableS2). Therefore, the selection toward ancestral allele do not carry any detrimental side
669 effects for fertility or malformations [84] and can be achieved without introgression.
670 In our design, all homozygous ancestral and the majority (79.7%) of heterozygous lambs could
671 be classified as short-tailed, while homozygous derived lambs are mostly (71.4%) but not
672 always long-tailed (**Table 6**). This could be caused by interaction (epistasis) with alleles at other
673 loci in the sheep genome or simply by the polygenic nature of the high proportion of additive
674 genetic variance which was still not explained by the mutations discovered here (0.898). In
675 addition, functional redundancy [75] and synergistic interaction [85] between the paralogus HOX
676 genes could contribute to the additional complexity of the phenotype. However, the genomic
677 region containing the HOXA (OAR04, 68 Mb), HOXC (OAR13, 132 Mb) and HOXD (OAR02,
678 132 Mb) gene clusters show no signals in the cLDLA analyses without (Model 3) and with
679 (Model 5) candidate mutations as a fixed effect (**Figure 1c** and **d**). Tacking together, to map
680 some remaining causal variants in long-tailed breeds, we will need a design with much higher
681 statistical power than the one carried out in the present study.
682 Our results provide a comprehensive insight into the genetic variance of tail length in long-
683 tailed Merino sheep and offer information towards direct gene-assisted selection for shorter
684 tails and thus contribute to animal welfare by avoiding tail docking and mulesing in the future.
685 Part of society, which is actively committed to animal welfare, frequently has prejudices against
686 genetic methods in general. Therefore, it should be pointed out once again that this is a natural
687 original genetic variant and that selection in favor of this variant serves to restore the most
688 natural original trait. We would not call it a "repair", but a "back to the roots". Additional to
689 commercial and animal welfare aspects this and follow-up study could contribute to a better
690 understanding of embryonal development too. According to Aires, et al. [86] quantitative
691 differences within the *Gdf11-Lin28-Hoxb13-Hoxc13* gene network might account for the tail
692 size variability observed among vertebrate species. Thereby, the determination of the tail length
693 could result from the relative intensity or the sequence of the individual network components.

694 The mechanisms regulating tail size are still not fully understood especially the pathways
695 downstream of *Lin28* and *Hox13* genes in the *Gdf11-Lin28-Hoxb13-Hoxc13* network.
696 Therefore, Aires, et al. [86] suggested testing the gene-network parameters in embryos of
697 vertebrate species with different tail sizes. The embryos of a sheep breed with an ancestral short
698 tail and a derived long tail are suitable candidates for studying the control of axis termination.
699 In the meantime, the mapping design could be extended and improved to map genes pointing
700 to further network candidates, possibly downstream mediators of the *HOXB13*.
701

702 Conclusions

703 From the results of our well-structured mapping population, we concluded that the tail length
704 is a highly heritable trait and depends on many loci with minor effects, whereas variations
705 around *HOXB13* cause the main effect in tail length. This is evident from the only slight
706 reduction in heritability after correcting for this major locus. To detect the additional causal loci
707 a more powerful design is needed. We have shown that variance component analysis in the
708 haplotype-based mixed linear model can be more successful than methods such as GWAS when
709 the number of phenotyped individuals and genotyped markers is not large enough for GWAS.
710 Further, our results indicated that second generation short reeds sequencing technology coupled
711 with the assembly errors can make finding promising structural candidate variants difficult and
712 thus visual examination of the targeted region should always be considered. However, long-
713 read sequencing technology such as PacBio and ONT have already proven to be effective in
714 identifying such SVs. Despite this, we were able to detect an insertion and a SNP within the
715 promotor and exon regions of *HOXB13* as the most plausible but possibly not sole cause for the
716 major effect. Furthermore, our results suggest sheep as model animals for deciphering the
717 mechanism of general interest, e.g. developmental biology and cancer. Finally, we clearly show
718 that selection for shorter tails in economically most important long-tailed Merino breeds is

719 possible without introgression and without negative side effects and that this selection is
720 ethically unproblematic as it leads to an increased frequency of the ancestral and thus for sheep
721 most natural allele.

722 Declarations

723 Ethics approval and consent to participate

724 The collection of blood samples for this study was approved by the ethics committee of the
725 Veterinary Faculty of LMU Munich.
726 All blood samples were taken according to best veterinary practice and under a permit from the
727 Government of Upper Bavaria (permit number: 55.2-1-54-2532.0-47-2016), or from the
728 Regional Council of Gießen, Hassia (KTV number: 19 c 20 15 h 02 Gi 19/1 KTV 22/2020).
729

730 Consent for publication

731 Not applicable
732

733 Availability of data and materials

734 The datasets generated during and/or analysed during the current study are available from the
735 corresponding author on reasonable request.
736

737 Competing interests

738 The authors declare that there is no conflict of interest.
739

740 Funding

741 DL was funded by a PhD Research Fellowship from the Tierzuchtforschung e.V. München.

Authors' contributions

DL analyzed and interpreted data and drafted the manuscript. EH and KE collected samples and phenotypes and assisted in drafting the manuscript. JK assisted in the interpretation of the analyses. DS and IR coordinated genotyping of the samples and provided data. CM provided expertise about the status and problems of modern sheep breeding and established contacts with breeders. GL provided samples and phenotypes. SK performed capture sequencing and assisted in drafting the manuscript. HB performed and coordinated capture sequencing. MU carried out data analyses and interpretation and assisted in drafting the manuscript. IM conceived and guided this study, provided analysis tools, analysed data and critically revised the manuscript. All authors read and approved the final manuscript.

Acknowledgements

The authors thank to breeder Hermann Stadler for making his sheep available for measuring and sampling.

References

1 Zeder, M. A. Domestication and early agriculture in the Mediterranean Basin: Origins, diffusion, and impact. *Proceedings of the National Academy of Sciences of the United States of America* **105**, 11597-11604, doi:10.1073/pnas.0801317105 (2008).

2 Arbuckle, B. S. & Atici, L. J. L. Initial diversity in sheep and goat management in Neolithic south-western Asia. **45**, 219-235, doi:10.1179/0075891413Z.00000000026 (2013).

3 Sherratt, A. J. W. a. The secondary exploitation of animals in the Old World. **15**, 90-104 (1983).

4 Shelton, M. Studies on tail length of Rambouillet and Mouflon sheep. *The Journal of heredity* **68**, 128-130, doi:10.1093/oxfordjournals.jhered.a108788 (1977).

5 Sutherland, M. A. & Tucker, C. B. The long and short of it: A review of tail docking in farm animals. *Applied Animal Behaviour Science* **135**, 179-191, doi:https://doi.org/10.1016/j.applanim.2011.10.015 (2011).

6 Hannemann, R., Bauer, B., Ganter, M. & Strobel, H. Schmerzhafte Eingriffe beim Schaf – Schwanzkupieren. Eine Übersicht. *Tierärztliche Praxis G: Großtiere/Nutztiere* **45**, 302-311, doi:10.15653/TPG-170354 (2017).

7 Bohte-Wilhelmus, D. I., De Haas, Y., Veerkamp, R. F. & Windig, J. J. in *Proceedings of the 9th world congress on genetics applied to livestock production, Leipzig, Germany, 1-6 August 2010.*

8 ThVO. (2017).

9

10 Lynch, J. J., Hinch, G. N. & Adams, D. B. *The behaviour of sheep: biological principles and implications for production*. 1 edn, (C.A.B. international, 1992).

11 James, P. J., Gare, D. R., Singh, A. W. & Ancell, P. M. Studies of the potential for breeding short tail Merinos. *Wool technology and sheep breeding* **38**, 106-111 (1990).

12 Greeff, J. C., Karlsson, L. J. E. & Schlink, A. C. Inheritance of tail length in Merino sheep. *Proc. Assoc. Advmt. Breed. Genet.* **21**, 237-240 (2015).

13 Branford Oltenacu, E. A. & Boylan, W. J. Inheritance of Tail Length in Crossbred Finnsheep. *Journal of Heredity* **65**, 331-334, doi:10.1093/oxfordjournals.jhered.a108543 (1974).

14 James, P., Ponzoni, R., Gare, D. & Cockrum, K. in *Proceedings of the Association for the Advancement of Animal Breeding and Genetics.* 404-407.

15 Scobie, D. & O'Connell, D. in *Proceedings of the New Zealand Society of Animal Production.* 195-198 (New Zealand Society of Animal Production; 1999).

16 Carter, A. H. Inherited taillessness in sheep. *New Zealand Ministry of Agriculture and Fisheries. Annual report of the research division.*, 44-45 (1976).

17 Zhi, D. *et al.* Whole Genome Sequencing of Hulunbuir Short-Tailed Sheep for Identifying Candidate Genes Related to the Short-Tail Phenotype. *G3 (Bethesda)* **8**, 377-383, doi:10.1534/g3.117.300307 (2018).

18 Hytönen, M. K. *et al.* Ancestral T-Box mutation is present in many, but not all, short-tailed dog breeds. *Journal of Heredity* **100**, 236-240, doi:10.1093/jhered/esn085 (2009).

19 Buckingham, K. J. *et al.* Multiple mutant T alleles cause haploinsufficiency of Brachyury and short tails in Manx cats. *Mamm Genome* **24**, 400-408, doi:10.1007/s00335-013-9471-1 (2013).

20 Indrebo, A. *et al.* A study of inherited short tail and taillessness in Pembroke Welsh corgi. *J Small Anim Pract* **49**, 220-224, doi:10.1111/j.1748-5827.2007.00435.x (2008).

21 Eck, K. *et al.* Morphometric measurements in lambs as a basis for future mapping studies. *Small Ruminant Research*, doi:10.1016/j.smallrumres.2019.04.007 (2019).

22 Illumina. *Data Sheet: Agrigenomics. OvineSNP50 Genotyping BeadChip*, <https://www.illumina.com> (2015).

23 Browning, B. L., Zhou, Y. & Browning, S. R. A One-Penny Imputed Genome from Next-Generation Reference Panels. *American journal of human genetics* **103**, 338-348, doi:10.1016/j.ajhg.2018.07.015 (2018).

24 Browning, S. R. & Browning, B. L. Haplotype phasing: existing methods and new developments. *Nature Reviews Genetics* **12**, 703-714 (2011).

25 Yang, J., Lee, S. H., Goddard, M. E. & Visscher, P. M. GCTA: a tool for genome-wide complex trait analysis. *American journal of human genetics* **88**, 76-82, doi:10.1016/j.ajhg.2010.11.011 (2011).

26 Yang, J. *et al.* Advantages and pitfalls in the application of mixed-model association methods. *Nat Genet* **46**, 100-106, doi:10.1038/ng.2876 (2014).

27 Xiong, X. *et al.* Genome-wide association analysis reveals genetic loci and candidate genes for meat quality traits in Chinese Laiwu pigs. *Mamm Genome* **26**, 181-190, doi:10.1007/s00335-015-9558-y (2015).

28 Meuwissen, T. H. E. *et al.* Fine mapping of a quantitative trait locus for twinning rate using combined linkage and linkage disequilibrium mapping. *Genetics* **161**, 373-379, doi:10.1093/genetics/161.1.373 (2002).

29 Kunz, E. *et al.* Confirmation of a non-synonymous SNP in PNPLA8 as a candidate causal mutation for Weaver syndrome in Brown Swiss cattle. *Genet Sel Evol* **48**, 21, doi:10.1186/s12711-016-0201-5 (2016).

30 Rothammer, S. *et al.* Remapping of the belted phenotype in cattle on BTA3 identifies a multiplication event as the candidate causal mutation. *Genetics Selection Evolution* **50**, 36, doi:10.1186/s12711-018-0407-9 (2018).

31 Rothammer, S. *et al.* Genome-wide QTL mapping of nine body composition and bone mineral density traits in pigs. *Genetics Selection Evolution* **46**, 68 (2014).

32 Müller, M.-P. *et al.* Genome-wide mapping of 10 calving and fertility traits in Holstein dairy cattle with special regard to chromosome 18. *Journal of dairy science* **100**, 1987-2006 (2017).

33 Powell, J. E., Visscher, P. M. & Goddard, M. E. Reconciling the analysis of IBD and IBS in complex trait studies. *Nat Rev Genet* **11**, 800-805, doi:10.1038/nrg2865 (2010).

34 Meuwissen, T. H. & Goddard, M. E. Prediction of identity by descent probabilities from marker-haplotypes. *Genet Sel Evol* **33**, 605-634, doi:10.1186/1297-9686-33-6-605 (2001).

35 Lee, S. H. & Van der Werf, J. H. J. Using dominance relationship coefficients based on linkage disequilibrium and linkage with a general complex pedigree to increase mapping resolution. *Genetics* **174**, 1009-1016, doi:10.1534/genetics.106.060806 (2006).

36 Gilmour, A. R. *et al.* ASReml User Guide Release 3.0. (VSN International Ltd, Hemel Hempstead, 2009).

37 Heuven, H. C. M., Bovenhuis, H., Janss, L. L. G. & van Arendonk, J. A. M. Efficiency of population structures for mapping of Mendelian and imprinted quantitative trait loci in outbred pigs using variance component methods. *Genetics Selection Evolution* **37**, 635-655, doi:10.1186/1297-9686-37-7-635 (2005).

38 Bland, J. M. & Altman, D. G. Multiple significance tests: the Bonferroni method. *BMJ* **310**, 170, doi:10.1136/bmj.310.6973.170 (1995).

39 van Ooijen, J. W. Accuracy of mapping quantitative trait loci in autogamous species. *Theor Appl Genet* **84**, 803-811, doi:10.1007/BF00227388 (1992).

40 qqman: Q-Q and Manhattan Plots for GWAS Data. v. R package version 0.1.4. (2017).

41 Jiang, Y. *et al.* The sheep genome illuminates biology of the rumen and lipid metabolism. *Science (New York, N.Y.)* **344**, 1168-1173, doi:10.1126/science.1252806 (2014).

42 Archibald, A. L. *et al.* The sheep genome reference sequence: a work in progress. *Animal genetics* **41**, 449-453, doi:10.1111/j.1365-2052.2010.02100.x (2010).

43 Yates, A. D. *et al.* Ensembl 2020. *Nucleic acids research* **48**, D682-d688, doi:10.1093/nar/gkz966 (2020).

44 *Genome–Assembly–NCBI*, <https://www.ncbi.nlm.nih.gov/assembly/GCF_000001635.27> (

45 *Genome–Assembly–NCBI*, <https://www.ncbi.nlm.nih.gov/assembly/GCF_000001405.39> (

46 Database resources of the National Center for Biotechnology Information. *Nucleic acids research* **46**, D8-d13, doi:10.1093/nar/gkx1095 (2018).

47 Chen, E. Y. *et al.* Enrichr: interactive and collaborative HTML5 gene list enrichment analysis tool. *BMC bioinformatics* **14**, 128, doi:10.1186/1471-2105-14-128 (2013).

48 Kuleshov, M. V. *et al.* Enrichr: a comprehensive gene set enrichment analysis web server 2016 update. *Nucleic acids research* **44**, W90-97, doi:10.1093/nar/gkw377 (2016).

49 Joshi NA, F. J. Sickle: A sliding-window, adaptive, quality-based trimming tool for FastQ files (Version 1.33). (2011).

50 B, B. FastQC: a quality control tool for high throughput sequence data. (2011).

51 Li, H. & Durbin, R. Fast and accurate short read alignment with Burrows-Wheeler transform. *Bioinformatics (Oxford, England)* **25**, 1754-1760, doi:10.1093/bioinformatics/btp324 (2009).

52 Li, H. *et al.* The Sequence Alignment/Map format and SAMtools. *Bioinformatics (Oxford, England)* **25**, 2078-2079, doi:10.1093/bioinformatics/btp352 (2009).

53 Institute, B. Picard toolkit. *Broad Institute, GitHub repository* (2019).

54 Auwera, G. d. & O'Connor, B. *Genomics in the Cloud: Using Docker, GATK, and WDL in Terra*. 1st Edition edn, (O'Reilly Media, 2020).

55 Danecek, P. *et al.* Twelve years of SAMtools and BCFtools. *GigaScience* **10**, doi:10.1093/gigascience/giab008 (2021).

56 Layer, R. M., Chiang, C., Quinlan, A. R. & Hall, I. M. LUMPY: a probabilistic framework for structural variant discovery. *Genome biology* **15**, R84, doi:10.1186/gb-2014-15-6-r84 (2014).

57 Rausch, T. *et al.* DELLY: structural variant discovery by integrated paired-end and split-read analysis. *Bioinformatics (Oxford, England)* **28**, i333-i339, doi:10.1093/bioinformatics/bts378 (2012).

58 Buels, R. *et al.* JBrowse: a dynamic web platform for genome visualization and analysis. *Genome biology* **17**, 66, doi:10.1186/s13059-016-0924-1 (2016).

59 Untergasser, A. *et al.* Primer3--new capabilities and interfaces. *Nucleic acids research* **40**, e115, doi:10.1093/nar/gks596 (2012).

60 R: A language and environment for statistical computing (R Foundation for Statistical Computing, Vienna, Austria. URL https://www.R-project.org/.).

61 McLaren, W. *et al.* The Ensembl Variant Effect Predictor. *Genome biology* **17**, 122, doi:10.1186/s13059-016-0974-4 (2016).

62 Altschul, S. F. *et al.* Basic local alignment search tool. *Journal of molecular biology* **215**, 403-410, doi:10.1016/s0022-2836(05)80360-2 (1990).

63 Yurtman, E. *et al.* Archaeogenetic analysis of Neolithic sheep from Anatolia suggests a complex demographic history since domestication. *Commun Biol* **4**, 1279, doi:10.1038/s42003-021-02794-8 (2021).

64 Li, R. *et al.* The first sheep graph-based pan-genome reveals the spectrum of structural variations and their effects on tail phenotypes. doi:10.1101/2021.12.22.472709 (2022).

65 Visscher, P. M. *et al.* Statistical power to detect genetic (co)variance of complex traits using SNP data in unrelated samples. *PLoS Genet* **10**, e1004269, doi:10.1371/journal.pgen.1004269 (2014).

66 Gluecksohn-Schoenheimer, S. The development of normal and homozygous brachy (T/T) mouse embryos in the extraembryonic coelom of the chick. *Proceedings of the National Academy of Sciences of the United States of America* **30**, 134-140 (1944).

67 Grüneberg, H. Genetical studies on the skeleton of the mouse: XXIII. The development of brachyury and anury. *Journal of Embryology and Experimental Morphology* **6**, 424-443 (1958).

68 Beddington, R. S. P., Rashbass, P. & Wilson, V. Brachyury-a gene affecting mouse gastrulation and early organogenesis. *Development*, 157-165 (1992).

69 Yoo, D. *et al.* The Genetic Origin of Short Tail in Endangered Korean Dog, DongGyeongi. *Sci Rep* **7**, 10048, doi:10.1038/s41598-017-10106-6 (2017).

70 Haworth, K. *et al.* Canine homolog of the T-box transcription factor T; failure of the protein to bind to its DNA target leads to a short-tail phenotype. *Mammalian Genome* **12**, 212-218 (2001).

71 Xu, X. *et al.* Whole Genome Sequencing Identifies a Missense Mutation in HES7 Associated with Short Tails in Asian Domestic Cats. *Sci Rep* **6**, 31583, doi:10.1038/srep31583 (2016).

72 Diaz-Cuadros, M., Pourquié, O. & El-Sherif, E. Patterning with clocks and genetic cascades: Segmentation and regionalization of vertebrate versus insect body plans. *PLoS Genet* **17**, e1009812, doi:10.1371/journal.pgen.1009812 (2021).

73 Lewis, E. B. A gene complex controlling segmentation in Drosophila. *Nature* **276**, 565-570, doi:10.1038/276565a0 (1978).

74 Wellik, D. M. Hox patterning of the vertebrate axial skeleton. *Developmental Dynamics* **236**, 2454-2463 (2007).

75 McIntyre, D. C. *et al.* Hox patterning of the vertebrate rib cage. **134**, 2981-2989, doi:10.1242/dev.007567 %J Development (2007).

76 Maconochie, M., Nonchev, S., Morrison, A. & Krumlauf, R. Paralogous Hox genes: function and regulation. *Annual review of genetics* **30**, 529-556, doi:10.1146/annurev.genet.30.1.529 (1996).

77 Casaca, A., Nóvoa, A. & Mallo, M. Hoxb6 can interfere with somitogenesis in the posterior embryo through a mechanism independent of its rib-promoting activity. *Development* **143**, 437-448 (2016).

78 Young, T. *et al.* Cdx and Hox genes differentially regulate posterior axial growth in mammalian embryos. *Developmental Cell* **17**, 516-526 (2009).

79 Economides, K. D., Zeltser, L. & Capecchi, M. R. Hoxb13 mutations cause overgrowth of caudal spinal cordand tail vertebrae. *Developmental Biology* **256**, 317-330 (2003).

80 Ouhtit, A. *et al.* Hoxb13, a potential prognostic biomarker for prostate cancer. *Front Biosci (Elite Ed)* **8**, 40-45, doi:10.2741/E749 (2016).

81 VanOpstall, C. *et al.* MEIS-mediated suppression of human prostate cancer growth and metastasis through HOXB13-dependent regulation of proteoglycans. *Elife* **9**, doi:10.7554/eLife.53600 (2020).

82 Johng, D. *et al.* HOXB13 interaction with MEIS1 modifies proliferation and gene expression in prostate cancer. *Prostate* **79**, 414-424, doi:10.1002/pros.23747 (2019).

83 Elbarbary, R. A., Lucas, B. A. & Maquat, L. E. Retrotransposons as regulators of gene expression. *Science (New York, N.Y.)* **351**, aac7247, doi:10.1126/science.aac7247 (2016).

84 Stoffel, M. A., Johnston, S. E., Pilkington, J. G. & Pemberton, J. M. Genetic architecture and lifetime dynamics of inbreeding depression in a wild mammal. *Nat Commun* **12**, 2972, doi:10.1038/s41467-021-23222-9 (2021).

85 Chen, F. & Capecchi, M. R. Targeted mutations in hoxa-9 and hoxb-9 reveal synergistic interactions. *Developmental biology* **181**, 186-196, doi:10.1006/dbio.1996.8440 (1997).

86 Aires, R. *et al.* Tail Bud Progenitor Activity Relies on a Network Comprising Gdf11, Lin28, and Hox13 Genes. *Dev Cell* **48**, 383-395.e388, doi:10.1016/j.devcel.2018.12.004 (2019).

87 Goujon, M. *et al.* A new bioinformatics analysis tools framework at EMBL-EBI. *Nucleic acids research* **38**, W695-699, doi:10.1093/nar/gkq313 (2010).

88 Sievers, F. *et al.* Fast, scalable generation of high-quality protein multiple sequence alignments using Clustal Omega. *Molecular systems biology* **7**, 539, doi:10.1038/msb.2011.75 (2011).

89 Li, X. *et al.* Whole-genome resequencing of wild and domestic sheep identifies genes associated with morphological and agronomic traits. *Nat Commun* **11**, 2815, doi:10.1038/s41467-020-16485-1 (2020).

90 Deng, J. *et al.* Paternal Origins and Migratory Episodes of Domestic Sheep. *Curr Biol* **30**, 4085-4095 e4086, doi:10.1016/j.cub.2020.07.077 (2020).

91 Heaton, M. P. *et al.* Using sheep genomes from diverse U.S. breeds to identify missense variants in genes affecting fecundity. *F1000Res* **6**, 1303, doi:10.12688/f1000research.12216.1 (2017).

92 Upadhyay, M. *et al.* The First Draft Genome Assembly of Snow Sheep (Ovis nivicola). *Genome Biol Evol* **12**, 1330-1336, doi:10.1093/gbe/evaa124 (2020).

93 Upadhyay, M. *et al.* Whole genome sequencing reveals a complex introgression history and the basis of adaptation to subarctic climate in wild sheep. *Mol Ecol* **30**, 6701-6717, doi:10.1111/mec.16184 (2021).

Figures

Figure 1: Results of performed mixed linear analyses presented as Manhattan Plots; (a) MLMA Model 1 with 45,114 markers no –log10(*p*-value) were above the suggestive line, the four markers with the lowest *p* values are shown; (b) MLMA Model 2 with 45,115 markers, the additionally added candidate locus on OAR11 shows genome-wide significance; (c) cLDLA Model 3 with 45,114 markers resulted in two genome-wide significant peaks on OAR2 and OAR11; (d) cLDLA Model 5 with 45,115 markers and candidate locus added as fix effect, the peak on OAR2 decreases below the genome-wide significance and the peak on OAR11 erases completely.

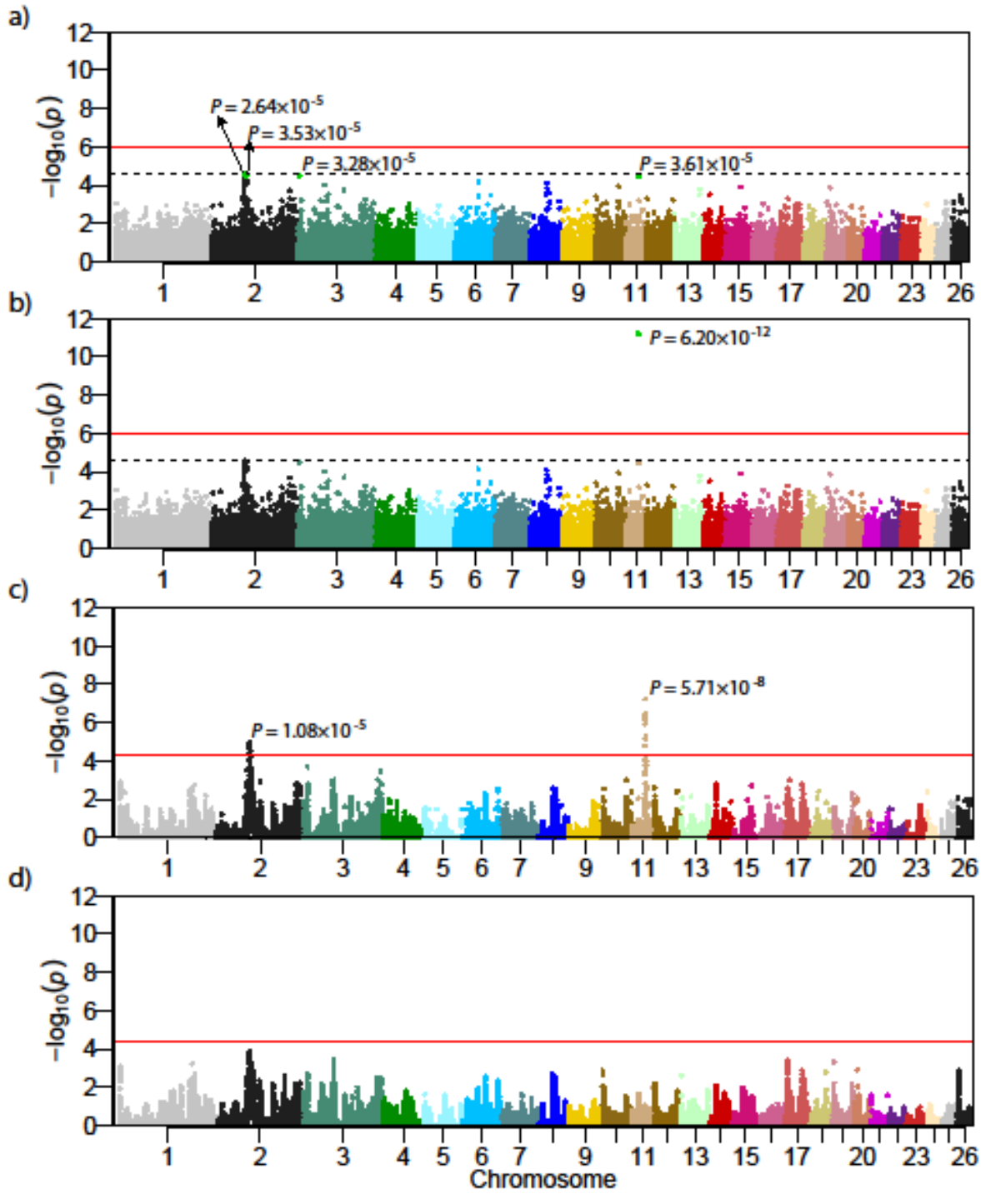

Figure 2: Amino acid sequence alignment of HOXB13 in multiple mammals. Positions of interest are highlighted. The asterisks present unique, the colons high similar and the single point moderate similar amino acids in every species on the respective position. To highlight the area of interest we used Clustal Omega [87,88] DA: Derived Allele, AA: Ancestral Allele

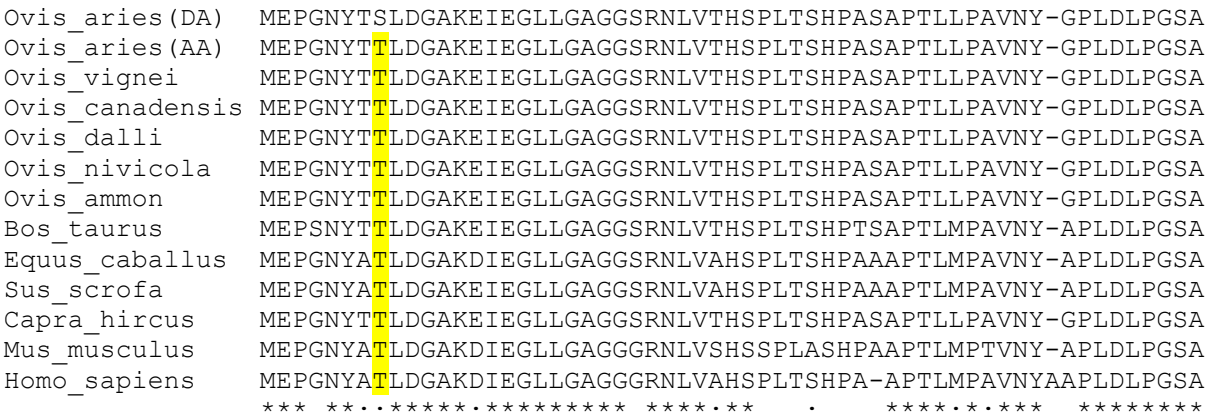

Figure 3: Screenshots showing insertions, position of the candidate SNP on 37,290,631 and extracts from the .ab1 trace files from sanger sequencing; a) Reads of the pooled sequenced long-tailed (above) and short- tailed (below) Merinolandschaf lambs mapped on assembly Oar_4.0, note the two clusters, cluster one is likely due to an assembly problem, cluster two represents an insertion shown in 34 of the 35 reads in the long-tailed group and in 13 of the 54 reads in the short-tailed group; b) shows the same groups mapped against the newest assembly ARS-UI_Ramb_v2.0, note the disappearance of cluster 1; c) sanger sequences for one homozygous derived (D/D), one heterozygous (A/D) and one homozygous ancestral (A/A) lamb around 40 bp before and after the breakpoint of the real insertion

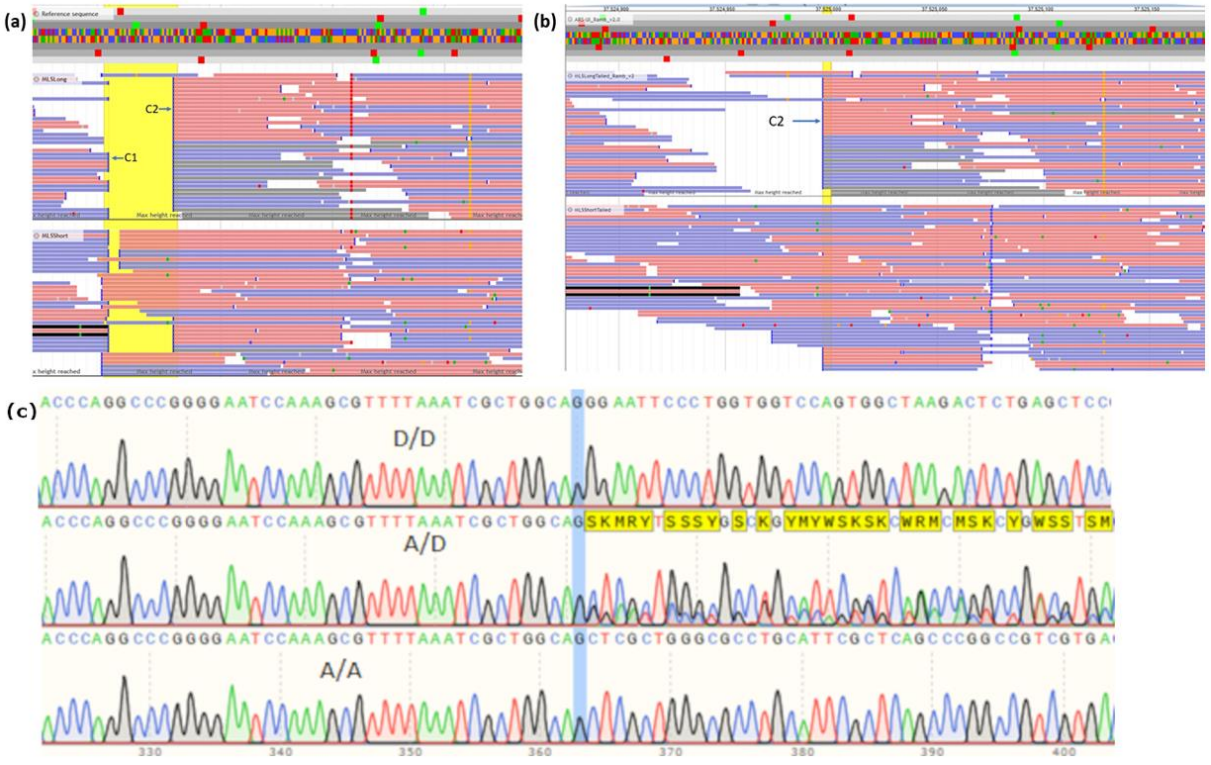

Tables

Table 1: Total number of visually inspected and sampled lambs at both sampling locations regarding to its phenotype

Sampling location		Visually inspected	Sampled			
			Total	Short	Long	Random
Lower Bavaria	**1. sampling**	2293	236	104	132	-
	2. sampling	110	102	-	-	102
JLU Giessen		102	24	19	5	-
Total		2505	362	123	137	102

Table 2: Mixed linear models used for association and combined linkage disequilibrium and linkage analysis. The fix and random effect are the overall mean (μ), sex, age, body weight (BW), withers height (WH), the vector of the additive effect of the candidate marker to be tested for association (a), the vector of random polygenic effects (u), the vector of random additive-genetic QTL effects (q) and the vector of random residual effects (e)

Analysis	Model name	Effects		Comment
		Fix	random	
MLMA	Model 1	μ, sex, age, BW, WH, a	u, e	
	Model 2	μ, sex, age, BW, WH, a	u, e	add one candidate locus as marker
cLDLA	Model 3	μ, sex, age, BW, WH	u, q, e	
	Model 4	μ, sex, age, BW, WH	u, q, e	add one candidate locus as marker
	Model 5	μ, sex, age, BW, WH, cSNP, a	u, q, e	add one candidate locus as fix effect

1006 **Table 3:** Run numbers and BioSample ID of different sheep breeds and there genotype for
1007 both candidate variants. Genotypes are homozygous ancestral (A/A), homozygous derived
1008 (D/D) and heterozygous (A/D)

Sample			Genotype		Submitted by
Breed	Run number	BioSample ID	SV	SNP	
Asiatic Mouflon	ERR157938	SAMEA2012637	A/A	A/A	Genoscope *
Asiatic Mouflon	ERR157930	SAMEA2012638	A/A	A/A	Genoscope *
Asiatic Mouflon	ERR157939	SAMEA2012639	A/A	A/D	Genoscope *
Asiatic Mouflon	ERR157942	SAMEA2012640	A/A	A/D	Genoscope *
Asiatic Mouflon	ERR157931	SAMEA2012641	A/A	D/D	Genoscope *
Asiatic Mouflon	ERR157932	SAMEA2012642	A/A	A/A	Genoscope *
Asiatic Mouflon	ERR157944	SAMEA1967031	A/A	A/A	Genoscope *
Asiatic Mouflon	ERR157935	SAMEA2012643	A/A	A/A	Genoscope *
Asiatic Mouflon	ERR332589	SAMEA2065600	A/A	A/A	Genoscope *
Asiatic Mouflon	ERR332575	SAMEA2065601	A/A	D/D	Genoscope *
Asiatic Mouflon	ERR332587	SAMEA2065602	A/A	A/A	Genoscope *
Asiatic Mouflon	ERR332582	SAMEA2065603	A/A	A/A	Genoscope *
Asiatic Mouflon	ERR332573	SAMEA1972234	A/A	A/D	Genoscope *
Asiatic Mouflon	ERR315509	SAMEA2065604	A/A	A/A	Genoscope *
Asiatic Mouflon	ERR466546	SAMEA2395410	A/A	A/A	Genoscope *
Asiatic Mouflon	ERR466544	SAMEA2395411	A/A	A/A	Genoscope *
Finnsheep	SRR11657543	SAMN14590314	A/A	A/A	Li, et al. [89]
Finnsheep	SRR11657544	SAMN14590313	A/D	A/D	Li, et al. [89]
Finnsheep	SRR11657545	SAMN14590312	A/A	A/A	Li, et al. [89]
Finnsheep	SRR11657546	SAMN14590311	A/A	A/A	Li, et al. [89]
Romanov	SRR12396891	SAMN15517583	A/A	A/D	Deng, et al. [90]
Romanov	SRR4291219	SAMN05216760	A/A	A/A	Heaton, et al. [91]
Romanov	SRR4291223	SAMN05216759	A/A	D/D	Heaton, et al. [91]
Romanov	SRR4291160	SAMN05216766	A/A	A/A	Heaton, et al. [91]
Swiss White Alpine	ERR3086436	SAMEA5239874	D/D	D/D	University of Bern**
Swiss White Alpine	ERR3086440	SAMEA5239878	D/D	D/D	University of Bern**
Swiss White Alpine	ERR3086476	SAMEA5239914	A/D	A/D	University of Bern**
Swiss White Alpine	ERR3086477	SAMEA5239915	A/D	A/D	University of Bern**
Rambouillet	SRR4291242	SAMN05216757	D/D	D/D	Heaton, et al. [91]
Rambouillet	SRR4291257	SAMN05216755	***	D/D	Heaton, et al. [91]
Rambouillet	SRR4291268	SAMN05216753	D/D	D/D	Heaton, et al. [91]
Rambouillet	SRR6305143	SAMEA104496890	A/D	A/D	Baylor College of Med.
Ancient DNA Seq	ERR3861593	SAMEA6516192	***	A/A	Yurtman, et al. [63]
Ancient DNA Seq	ERR3861592	SAMEA6516191	***	A/A	Yurtman, et al. [63]
Ovis ammon	SRR8560952	SAMN10915547	A/A	A/A	CAAS****
Ovis ammon	SRR8560953	SAMN10915548	A/A	A/A	CAAS****
Ovis ammon	SRR9222805	SAMN11979390	A/A	A/A	CAAS****
Ovis ammon	SRR9222806	SAMN11979389	A/A	A/A	CAAS****
Ovis ammon	SRR9222807	SAMN11979391	A/A	A/A	CAAS****
Ovis canadensis	SRR501858	SAMN01000748	A/A	A/A	Baylor College of Med.
Ovis canadensis	SRR501895	SAMN01000746	A/A	A/A	Baylor College of Med.
Ovis canadensis	SRR501898	SAMN01000747	A/A	A/A	Baylor College of Med.

Ovis dalli	SRR501847	SAMN01000785	A/A	A/A	Baylor College of Med.
Ovis dalli	SRR501897	SAMN01000764	A/A	A/A	Baylor College of Med.
Ovis vignei	ERR454945	SAMEA2358291	A/A	A/A	Genoscope *
Ovis vignei	ERR454946	SAMEA2358287	A/A	A/A	Genoscope *
Ovis vignei	ERR454947	SAMEA2358290	A/A	A/A	Genoscope *
Ovis vignei	ERR454948	SAMEA2358289	A/A	A/A	Genoscope *
Ovis vignei	ERR454950	SAMEA2358291	A/A	A/A	Genoscope *
Ovis nivicola	ERR4161992	SAMEA6833340	A/A	A/A	Upadhyay, et al. [92]
Ovis nivicola	ERR6667562	SAMEA8657697	A/A	A/A	Upadhyay, et al. [93]
Ovis nivicola	ERR6668200	SAMEA8657699	A/A	A/A	Upadhyay, et al. [93]
Ovis nivicola	ERR6668794	SAMEA8657700	A/A	A/A	Upadhyay, et al. [93]
Ovis nivicola	ERR6667561	SAMEA8657698	A/A	A/A	Upadhyay, et al. [93]
Ovis nivicola	ERR5858461	SAMEA8657696	A/A	A/A	Upadhyay, et al. [93]

1009

1010 * Sequenced as part of the NextGen project
1011 ** Institute of Genetics
1012 *** No reads mapped
1013 **** Institute of Animal Science of CAAS

1014 **Table 4**: Genes on OAR11 between positions 37,000,925 bp and 37,521,490 bp as well as the
1015 genome-wide significant peaks of cLDLA Model 3 and 4

Gene	Name	Start (bp)	End (bp)
IGF2BP1	insulin like growth factor 2 mRNA binding protein 1	37,009,695	37,032,963
GIP	gastric inhibitory polypeptide	37,074,497	37,079,791
SNF8	SNF8, ESCRT-II complex subunit	37,093,635	37,101,565
UBE2Z	ubiquitin conjugating enzyme E2 Z	37,104,244	37,117,532
QTL-Peak	Peak of cLDLA Model 3	37,111,462	
ATP5G1	ATP synthase	37,125,809	37,128,277
CALCOCO2	calcium binding and coiled-coil domain 2	37,179,738	37,202,548
TTLL6	tubulin tyrosine ligase like 6	37,221,445	37,263,708
HOXB13	homeobox B13	37,290,203	37,292,513
QTL-Peak	Peak of cLDLA Model 4	37,311,842	
HOXB9	homeobox B9	37,365,122	37,369,564
HOXB8	homeobox B8	37,376,709	37,378,201
HOXB7	homeobox B7	37,381,261	37,384,010
HOXB6	homeobox B6	37,391,399	37,395,989
HOXB5	homeobox B5	37,397,814	37,404,968
HOXB3	homeobox B3	37,437,808	37,439,623
HOXB2	homeobox B2	37,445,188	37,448,075
HOXB1	homeobox B1	37,457,621	37,460,240

1016

1017

1018

1019

1020

1021

1022

Table 5*:* Genes on OAR2 between positions 93,441,900 bp and 96,402,884 bp as well as the genome-wide significant peak of cLDLA Model 3

Gene	**Name**	**Start (bp)**	**End (bp)**
CAAP1	caspase activity and apoptosis inhibitor 1	94,480,790	94,556,081
QTL-Peak	Peak of cLDLA Model 3	94,538,115	
PLAA	phospholipase A2 activating protein	94,567,698	94,605,168
IFT74	intraflagellar transport 74	94,607,523	94,708,596
LRRC19	leucine rich repeat containing 19	94,629,884	94,643,326
TEK	TEK receptor tyrosine kinase	94,739,266	94,838,005
EQTN	Equatorin	94,900,676	94,917,170
MOB3B	MOB kinase activator 3B	94,934,882	95,077,788
IFNK	interferon kappa	95,145,920	95,147,256
C9ORF72	C9orf72-SMCR8 complex subunit	95,183,641	95,202,857
LINGO2	leucine rich repeat and Ig domain containing 2	95,627,231	95,629,051

Table 6: The number of individuals, mean and SD of tail length, QTL effects and polygenic effects of the different genotype groups. The groups are homozygous ancestral (A/A), homozygous derived (D/D) and heterozygous (A/D)

Genotype	Count			Tail length		QTL effect		Polygenic effect	
	all	short	Long	Mean	SD	Mean	SD	Mean	SD
D/D	210	70	150	31.5	5.56	0.68	1.27	1.12	3.56
A/D	118	94	24	25.7	3.66	-1.3	0.89	-1.61	2.96
A/A	24	24	0	24.1	1.34	-2.92	0.71	-2.19	1.52